

observed. The common feature for all the nanoparticles present in the soot is the strong phase separation between chemical species (B and N on one side and C on the other side). Therefore, it is realistic to propose nanotube-based devices compatible with this phase separation, such as axial BN-C heterojunctions or superlattices (10), whereas the production of homogeneous nanotubes with an ordered BC₂N structure (11) appears more difficult to control, at least under arc-discharge conditions.

The clear phase separation observed between BN layers and C layers raises the question of the growth mechanism itself. A segregation process taking place by diffusion between layers after the particles are formed can be ruled out because of the very slow interlayer diffusion rates. A workable hypothesis is that BN particles grow first and then go through a carbon-rich region of the plasma, leading to a carbon coating on the surface of all particles. For the C-BN-C sandwich geometry observed in most tubes, it must then be assumed that the coating is also efficient for the inner surface of the tube and that it occurs by diffusion of carbon atoms from the open-ended tip of the tube. A similar scenario has been reported for the filling and coating of carbon nanotubes by molten V₂O₅ (19). The inner coating of the polyhedral nanoparticles is prevented by their close-shelled nature. In the case of the tubes, another scenario can be envisioned in which the BN shells and the carbon shells grow simultaneously. Ab initio molecular dynamics simulations of the growth mechanism of a bilayer tube have shown that lip-lip interactions are important and that adjacent layers are connected by bridges saturating the dangling bonds (20). Fast diffusion processes leading to phase separation could take place within these bridges.

The sandwich C-BN-C geometry found for some tubes closely resembles the metal-insulator-metal geometry of the memory device proposed for nanotube applications (6) as well as that of a coaxial nanocable. The key to producing mixed nanotubes while avoiding the dominant formation of carbon tubes is to control the vaporization of carbon. Taking advantage of the natural phase separation between BN and C under arc-discharge conditions should make it possible to achieve the controlled production of nanotubes in which BN and C are alternated either between layers or within the layers. Measuring the electrical properties of these composite tubes—as was recently done in the case of pure carbon tubes, including single-wall tubes (21)—is of particular interest.

REFERENCES AND NOTES

1. S. Iijima, *Nature* **354**, 54 (1991).
2. D. Ugarte, *ibid.* **359**, 707 (1992).
3. L. Boulanger, F. Willaime, M. Cauchetier, in *Proceedings of the 13th International Conference on Electron Microscopy*, vol. IIIA, B. Jouffrey and C. Colliex, Eds. (Editions de Physique, Paris, 1994), pp. 315–316; L. Boulanger, B. Andriot, M. Cauchetier, F. Willaime, *Chem. Phys. Lett.* **234**, 227 (1995); F. Banhart, M. Zwanger, H. J. Muhr, *ibid.* **231**, 98 (1994).
4. N. G. Chopra *et al.*, *Science* **269**, 966 (1995); M. Terrones *et al.*, *Chem. Phys. Lett.* **259**, 568 (1996).
5. A. Loiseau, F. Willaime, N. Demoncey, G. Hug, H. Pascard, *Phys. Rev. Lett.* **76**, 4737 (1996).
6. M. S. Dresselhaus, G. Dresselhaus, P. C. Eklund, *Science of Fullerenes and Carbon Nanotubes* (Academic Press, London, 1996), p. 903.
7. N. Hamada, S. Sawada, A. Oshiyama, *Phys. Rev. Lett.* **68**, 1579 (1992); R. Saito, M. Fujita, G. Dresselhaus, M. S. Dresselhaus, *Phys. Rev. B* **46**, 1804 (1992).
8. P. Lambin, A. Fonseca, J. P. Vigneron, J. B. Nagy, A. A. Lucas, *Chem. Phys. Lett.* **245**, 85 (1995); R. Saito, G. Dresselhaus, M. S. Dresselhaus, *Phys. Rev. B* **53**, 2044 (1996); L. Chico, L. X. Benedict, S. G. Louie, M. L. Cohen, *Phys. Rev. Lett.* **76**, 971 (1996).
9. X. Blase, J.-C. Charlier, A. De Vita, R. Car, *Appl. Phys. Lett.* **70**, 197 (1997); E. G. Gal'pern, V. V. Pinyaskin, I. V. Stankevish, L. A. Chernozatonskii, *J. Phys. Chem. B* **101**, 705 (1997).
10. X. Blase, A. Rubio, S. G. Louie, M. L. Cohen, *Europhys. Lett.* **28**, 335 (1994).
11. Y. Miyamoto, A. Rubio, M. L. Cohen, S. G. Louie, *Phys. Rev. B* **50**, 18360 (1994); *ibid.*, p. 4976.
12. O. Stephan *et al.*, *Science* **266**, 1683 (1994).
13. Z. Weng-Sieh *et al.*, *Phys. Rev. B* **51**, 11229 (1995).
14. Ph. Redlich *et al.*, *Chem. Phys. Lett.* **260**, 465 (1996).
15. Taking advantage of the gas ambient as a constituent has led to the successful synthesis of BN tubes (5) and doping of carbon tubes (12) in arc methods. It may be possible to control the chemical composition of the tubes by monitoring the gas composition in the chamber.
16. A scanning transmission electron microscope (STEM VG-HB501) equipped with a parallel detector (Gatan PEELS 666) was operated at 100 kV. See, for example, C. Colliex, *J. Electron Microsc.* **45**, 44 (1996).
17. All the K-edge weights are normalized by hydrogenic cross section and the elastic peak for each element; therefore, the profiles are proportional to the numbers of selected atoms. The smallest probe (0.5 nm) was used. Acquisition time for the EELS was reduced to 1 s to prevent beam-induced effects at the cost of a reduction of signal-to-noise ratio in N K-edge counts in some cases. For details, see R. F. Egerton, *EELS in the Electron Microscope* (Plenum, New York, ed. 2, 1996); C. Colliex, in *EELS in Materials Science*, M. M. Disko, C. C. Ahn, B. Fultz, Eds. (TMS, Minerals, Metals, Materials Society, Warrendale, PA, 1992), pp. 86–106.
18. O. Stephan, P. M. Ajayan, C. Colliex, F. Cyrot-Lackmann, E. Sandre, *Phys. Rev. B* **53**, 13824 (1996).
19. P. M. Ajayan, O. Stephan, Ph. Redlich, C. Colliex, *Nature* **375**, 564 (1995).
20. J.-C. Charlier, A. De Vita, X. Blase, R. Car, *Science* **275**, 646 (1997).
21. S. J. Tans *et al.*, *Nature* **386**, 474 (1997).
22. We thank X. Deschanel (CEA/Saclay) for providing hafnium diboride rods. Partially supported by NEDO international joint research grant "Novel Nanotubular Materials: Production, Characterization and Properties."

7 July 1997; accepted 9 September 1997

Nanotubule-Based Molecular-Filtration Membranes

Kshama B. Jirage, John C. Hulthen, Charles R. Martin*

Polymeric membranes that contain a collection of monodisperse gold nanotubules, with inside diameters of molecular dimensions (less than 1 nanometer), were used in a simple membrane-permeation experiment to cleanly separate small molecules on the basis of molecular size. For example, when such a membrane was presented with an aqueous feed solution containing pyridine (molecular weight 79) and quinine (molecular weight 324), only the smaller pyridine molecule was transported through the nanotubules and into a receiver solution on the other side of the membrane.

Membrane-based chemical separations are potentially more economical and easier to implement than competing separations technologies, but membranes with higher transport selectivities are required (1–5). Chemical features of the membrane, and of the molecule to be selectively transported, that can be exploited to enhance transport selectivity include charge, chemical interactions, and molecular size. The ideal approach for implementing molecular size-based transport selectivity would be to de-

sign a synthetic membrane that has a collection of monodisperse nanopores, of molecular dimensions, that span the complete thickness of the membrane. If this could be accomplished, one could envision general "molecular filters" that could be used in a simple membrane-permeation experiment to cleanly separate small molecules on the basis of size. We describe such membranes here.

This idea of using membranes to filter molecules on the basis of size is not without precedent. Dialysis is used routinely to separate low-molecular weight species from macromolecules (6). In addition, nanofiltration membranes are known for certain small-molecule separations (such as water

Department of Chemistry, Colorado State University, Fort Collins, CO 80523, USA.

*To whom correspondence should be addressed at cmartin@lamar.colostate.edu

purification) (7), but such membranes typically combine both size and chemical transport selectivity and are particularly designed for the separation involved. And, although zeolites have molecule-sized pores, they are not typically used for membrane-based chemical separations (8). Hence, in spite of the importance of the concept, synthetic membranes that contain a collection of monodisperse, molecule-sized pores that can be used as molecular filters to separate small molecules on the basis of size are currently not available.

The membranes described here were prepared from polycarbonate filters (Poretics) that contain monodisperse, cylindrical pores 30 nm in diameter (9, 10). Martin and co-workers have shown (9, 11, 12) that an electroless plating procedure can be used to deposit an Au nanotubule within each pore (Fig. 1A). The inside diameter (ID) of these Au nanotubules can be varied by varying the plating time [see figure 1 in (11)]. At sufficiently long plating times, Au nanotubules with IDs of molecular dimensions (<1 nm) are obtained (11, 13).

We have since discovered that the shape of the Au nanotubule can be changed by varying the rate of the plating reaction. When high plating rates were used (14), Au was preferentially deposited on the faces of the membrane, and nanotubules with bottlenecks at both ends but a larger ID in the middle (Fig. 1B) were obtained. Such bottleneck tubules are a form of ultrathin film composite membrane (3, 7) and should provide high permeate flux without sacrificing

transport selectivity. This is so because selectivity should be determined by permeation through the bottleneck, but overall flux is determined by permeation in the larger ID tubule that spans the membrane (see below).

We show here that membranes containing such bottleneck nanotubules can be used to filter molecules on the basis of size. We mounted the nanotubule membrane in a U-tube permeation cell such that the membrane separated a feed solution from a permeate solution (15). The feed solution was equimolar in two compounds of different molecule size. We call these the "smaller" and the "larger" molecules; three "smaller molecule–larger molecule pairs" were investigated here (Fig. 2, A to C). The permeate solution, initially just pure water, was periodically assayed for the presence of both the smaller and the larger molecules. In all three cases (Fig. 2), easily measurable quantities of the smaller molecule were obtained in the permeate solution, but the larger molecule was completely undetectable.

We began our studies, however, with simpler single-molecule permeation experiments (16). These experiments were done in the same U-tube permeation cell (15), but the feed solution contained only one of the molecules of the smaller molecule–larger

er molecule pair. The flux of this molecule across the nanotubule membrane was determined, and then in a separate experiment the flux of the other molecule of the pair was measured (17). The objective was to explore the effect of nanotubule ID on transport rate and selectivity. Nanotubules with the more conventional shape (Fig. 1A) were used for these preliminary studies.

Results of such single-molecule permeation experiments, based on the use of the methyl viologen (MV^{2+}) Ru(II)tris(2,2'-bipyridine) [$Ru(bpy)_3^{2+}$] pair (Fig. 2A) and membranes with four different nanotubule IDs (13), are shown in Fig. 3, A to D. The slopes of these permeation curves define the fluxes of MV^{2+} and $Ru(bpy)_3^{2+}$ across the membrane. One can obtain a permeation selectivity coefficient (α_i) (18) by dividing the MV^{2+} flux by the $Ru(bpy)_3^{2+}$ flux.

The data in Fig. 3 may be summarized as follows: (i) Even for the nanotubules with the largest ID investigated (5.5 nm), α_i was substantially greater than the ratio of the diffusion coefficients (D) for these molecules in aqueous solution [$\alpha_i = 50$; ratio of diffusion coefficients = 1.5 (19)]. Hence, size-based sieving occurred in these large ID (\gg molecular dimensions) nanotubules (20). (ii) As the nanotubule ID decreased, the fluxes for both molecules decreased; however, the flux of the larger $Ru(bpy)_3^{2+}$

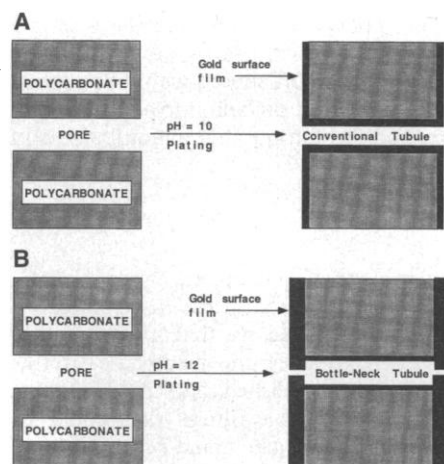


Fig. 1. Schematic illustrations of the shapes of the Au nanotubules that we obtained by doing the electroless Au plating (9) at (A) pH = 10 and (B) pH = 12. The higher pH causes bottleneck tubules. The tubules plated at the lower pH also have some of this bottleneck character [see (11)]. Hence, the depictions in both (A) and (B) are approximate and serve to illustrate the conceptual differences between the two types of nanotubules investigated here.

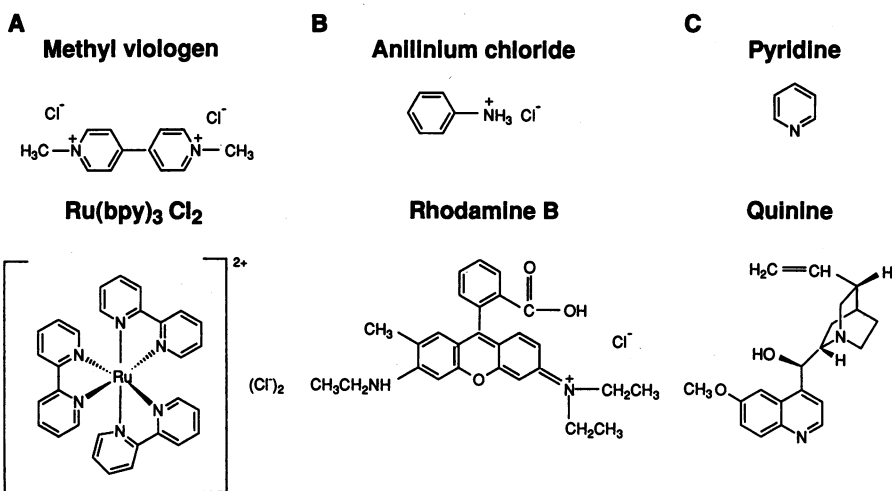


Fig. 2. Chemical structures and approximate relative sizes of the three pairs of molecules studied here: (A) methyl viologen chloride and Ru tris(2,2'-bipyridine) chloride, (B) anilinium chloride and rhodamine B chloride, and (C) pyridine and quinine. The charges on the molecules of each pair are the same. Because the permeate solution was initially just pure water, the cations [(A) and (B)] come across the membrane with their charge-balancing anions.

Table 1. Minimal selectivity coefficients for the three different small molecule–large molecule pairs.

Small molecule	Large molecule	Minimal selectivity coefficients
Methyl viologen chloride	Ruthenium tris(2,2'-bipyridine) chloride	1,500
Pyridine	Quinine	15,000
Anilinium chloride	Rhodamine B chloride	130,000

decreased more rapidly. As a result, α_i increased with decreasing nanotubule ID (21). Values for the nanotubule membranes with IDs of 5.5, 3.2, and 2.0 nm are $\alpha_i = 50$, 88, and 172, respectively. (iii) The nanotu-

bule membrane with the smallest ID (Fig. 3D) showed a measurable flux for MV^{2+} , but the larger $Ru(bpy)_3^{2+}$ could not be detected in the permeate solution, even after a 2-week permeation time.

Although the results of these experiments were encouraging in terms of selectivity, the fluxes were low. We expected that higher fluxes could be obtained from the bottleneck nanotubule membranes (Fig. 1B). A simple single-molecule permeation experiment was done to demonstrate the bottleneck character of these nanotubules. The MV^{2+} flux in a typical bottleneck membrane is $19 \text{ nmol hour}^{-1} \text{ cm}^{-2}$. When the surface Au layer containing the bottleneck (Fig. 1B) was removed (12), the flux increased by one order of magnitude to $180 \text{ nmol hour}^{-1} \text{ cm}^{-2}$. When the second surface Au layer was removed, the flux again increased by an order of magnitude. That these very thin surface Au layers (150 nm versus $16 \mu\text{m}$ for the polycarbonate membrane) can have such a dramatic effect on the flux clearly shows that flux-limiting constrictions are present in the surface layers (Fig. 1B).

It is also important to prove that these bottleneck membranes can have the same selectivity but higher flux than membranes containing the conventional nanotubules (Fig. 1A). To demonstrate this point, we compared the rate and selectivity of transport across a conventional and a bottleneck membrane (22). Both membranes were able to cleanly separate MV^{2+} from $Ru(bpy)_3^{2+}$ in the two-molecule permeation experiment (see below). Hence, these membranes showed comparable, excellent selectivity. However, as expected, the flux of MV^{2+} across the bottleneck nanotubule membrane was dramatically higher than that of the conventional nanotubule membrane (14 versus $0.07 \text{ nmol hour}^{-1} \text{ cm}^{-2}$).

We now turn to the more interesting case of having both molecules of a pair in the feed solution together. These experiments were done only on bottleneck nanotubule membranes that showed $\alpha_i = \infty$

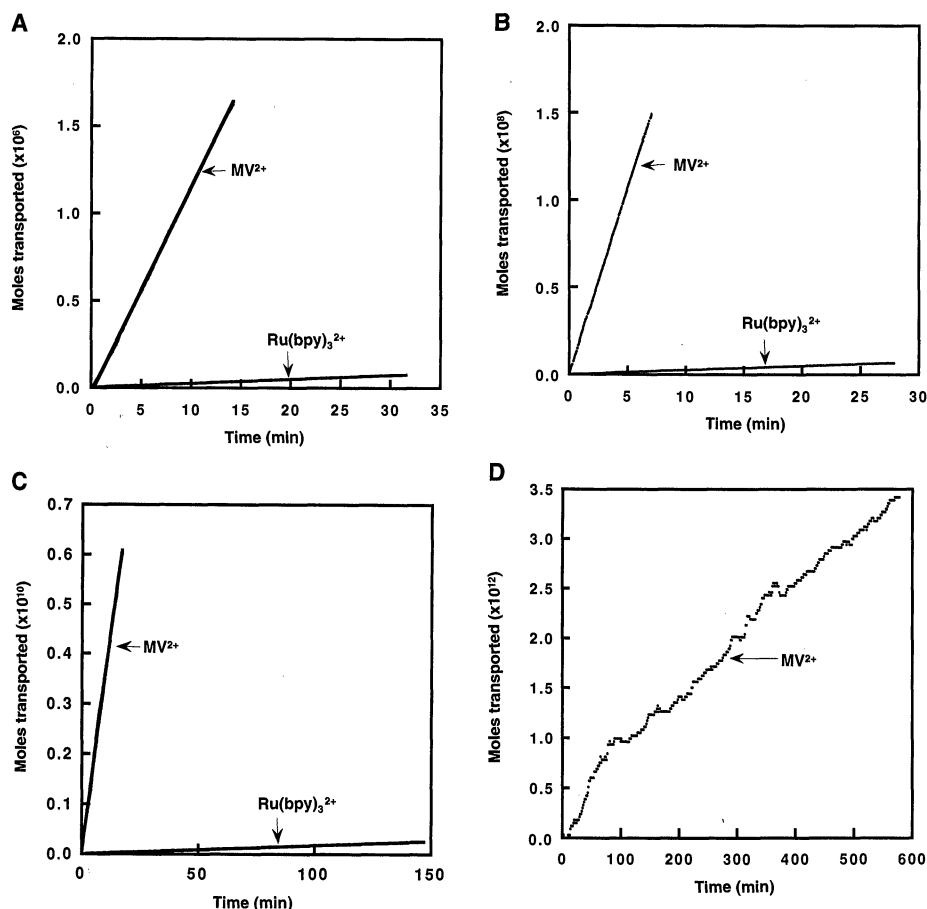


Fig. 3. Amounts of moles of MV^{2+} and $Ru(bpy)_3^{2+}$ transported versus time. Membranes contained nanotubules as depicted in Fig. 1A with diameters (13) of (A) 5.5 nm, (B) 3.2 nm, and (C) 2.0 nm. The nanotubule diameter in (D) was too small to measure by the gas-permeation method (diameter $< 0.6 \text{ nm}$). Only MV^{2+} was transported through this membrane. The data in (D) show more noise than the data in (A), (B), and (C) because the flux is lower.

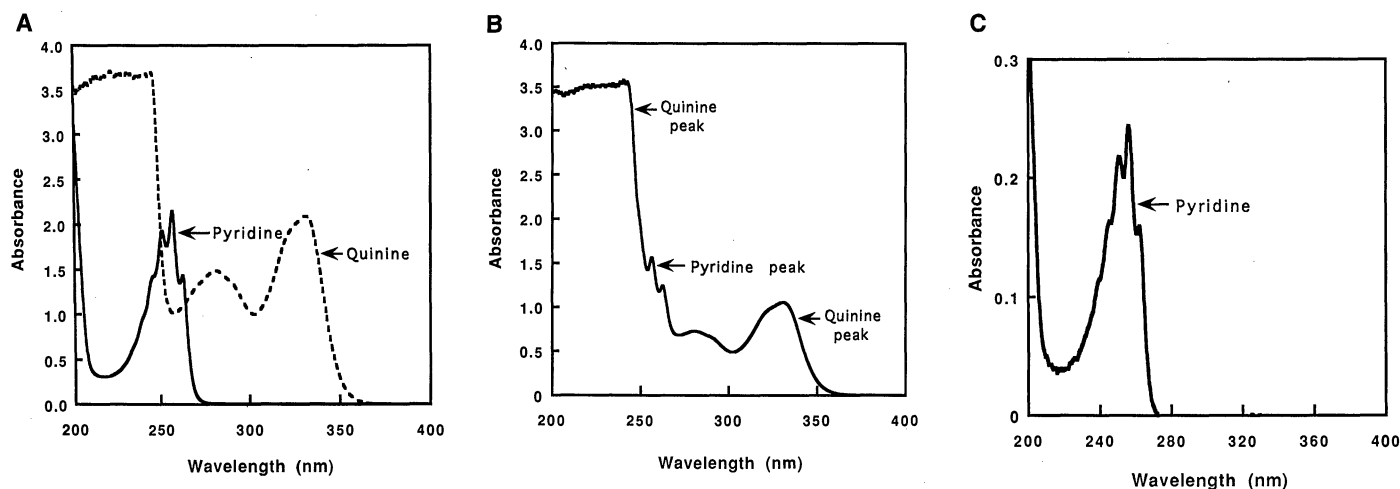


Fig. 4. Absorption spectra for (A) 0.5 mM pyridine and 0.5 mM quinine, (B) the pyridine-quinine feed solution (both molecules 0.25 mM), and (C) permeate after transport for 72 hours through a bottleneck nanotubule membrane (22).

(22). Typical results, for the pyridine-quinine pair, are shown in Fig. 4. The absorption spectra for 0.5 mM quinine and for 0.5 mM pyridine are shown in Fig. 4A. Pyridine shows a characteristic peak at ~ 252 nm. Quinine shows a much more intense band centered at 225 nm and two other bands at ~ 280 and ~ 330 nm.

The absorption spectrum for the feed solution used in the permeation experiment is shown in Fig. 4B. Although both molecules are present in solution at the same concentration, the higher absorbance of the quinine nearly swamps out the 252-nm peak of the pyridine. The absorption spectrum of the permeate solution after 72 hours is shown in Fig. 4C. In spite of the higher absorbance of the quinine (larger molecule), only the peak for the pyridine (smaller molecule) is seen in this spectrum. The very intense quinine band centered at 225 nm is absent. To our ability to make the measurement, this bottleneck nanotubule membrane has filtered these two molecules on the basis of molecular size (Fig. 4C).

To verify this point, we used a much more sensitive analytical method, fluorescence (23), to search for traces of quinine in the permeate solution. The magnitude of the absorbance in Fig. 4C indicates that the pyridine concentration in the permeate is 7×10^{-5} M. With fluorescence analysis (23), it is possible to detect 5×10^{-9} M quinine in the presence of 7×10^{-5} M pyridine. However, no quinine fluorescence could be detected from the permeate solution. These data show that, to our (now much more sensitive) ability to make the measurement, this membrane has cleanly separated these two molecules and that if any quinine is present in the permeate solution, its concentration is less than 5×10^{-9} M.

These analytical data can be used to calculate a minimal selectivity coefficient, α_{\min} . Because the concentration of the smaller molecule in the permeate solution was 7×10^{-5} M and the concentration of the larger molecule (if present at all) must be less than 5×10^{-9} M, the minimal selectivity coefficient for the pyridine-quinine pair is $\alpha_{\min} = 15,000$. Minimal selectivity coefficients obtained in this way (24) for the other pairs are shown in Table 1. In all three cases, the larger molecule was undetectable in the permeate solution.

Nishizawa *et al.* have demonstrated that these Au nanotubule membranes can show charge-based transport selectivity (9), and we have shown here that these membranes can also have molecular size-based selectivity. It seems likely that chemical transport selectivity can also be introduced. Hence, these nanotubule membranes hold promise for the development of highly selective membranes for chemical separations.

REFERENCES AND NOTES

- J. M. S. Hennis and M. K. Tripodi, *Science* **220**, 11 (1983).
- P. H. Abelson, *ibid.* **224**, 1421 (1989).
- C. Liu and C. R. Martin, *Nature* **352**, 50 (1991).
- "Membrane Separation Systems—A Research Needs Assessment" (Department of Energy Rep. DE90-01170, U.S. Department of Energy, Washington, DC, April 1990).
- R. W. Spillman, *Chem. Eng. Prog.* **85**, 41 (1989).
- M. Mulder, *Basic Principles of Membrane Technology* (Kluwer Academic, Dordrecht, Netherlands, 1990), pp. 260–262.
- R. J. Peterson, *J. Membr. Sci.* **83**, 81 (1993).
- Zeolites are used for sorption-based separations, for example, industrial O_2 - N_2 separation. In addition, there have been a number of recent attempts to make zeolite membranes. See Y. Yan *et al.*, *J. Chem. Soc. Chem. Commun.* **1995**, 227 (1995).
- M. Nishizawa, V. P. Menon, C. R. Martin, *Science* **268**, 700 (1995).
- C. R. Martin, *ibid.*, **266**, 1961 (1994).
- Y. Kobayashi and C. R. Martin, *J. Electroanal. Chem.*, in press.
- V. P. Menon and C. R. Martin, *Anal. Chem.* **67**, 1920 (1995).
- We approximated the IDs of tubules using a gas permeation method (9).
- In our earlier studies, we used a plating bath at pH = 10 (9, 11). Higher plating rates can be achieved with the same plating bath at pH = 12.
- B. B. Lakshmi and C. R. Martin, *Nature* **388**, 758 (1997).
- Such single-molecule permeation experiments are used routinely. See, for example, R. V. Parthasarathy, V. P. Menon, C. R. Martin, *Chem. Mater.* **9**, 560 (1997).
- We determined the flux by continuously monitoring the ultraviolet (UV) absorbance of the permeate solution while passing the permeate through a UV detector.
- The subscript "i" is for "ideal" and signifies that these coefficients were obtained by single-molecule permeation experiments. See (16).
- D values are from Z. Prat, Y.-M. Tricot, and I. Rubinstein [*J. Electroanal. Chem.* **315**, 225 (1991)] (MV^{2+}) and C. R. Martin, I. Rubinstein, and A. J. Bard [*ibid.* **115**, 267 (1983)] [$Ru(bpy)_3^{2+}$].
- Similar sieving was observed in radiotracer self-diffusion experiments on lightly etched films prepared by the track-etch process [T. K. Rostovtseva *et al.*, *J. Membr. Biol.* **151**, 29 (1996)]. However, molecular filtration of the type described here could not be observed.
- Although α_i , in general, increased with decreasing tubule ID, an interesting anomaly was observed for two membranes with tubule IDs between those in Fig. 3, C and D. The α_i values for these membranes were lower than the $\alpha_i = 172$ observed in Fig. 3C. We are now exploring the genesis of this anomaly.
- Because of the nonuniform shape of the bottleneck tubules (Fig. 1B), it is difficult to extract an ID with the gas-flux method (9). All bottleneck membranes were plated from pH = 12 bath for a duration of 8 hours.
- Quinine was excited at an excitation wavelength (λ_{ex}) of 308 nm and detected at an emission wavelength (λ_{em}) of 403 nm.
- The minimal quantity of $Ru(bpy)_3^{2+}$ that could be detected was determined by fluorescence: $\lambda_{ex} = 286$ nm; $\lambda_{em} = 594$ nm. The concentration of MV^{2+} was determined by UV absorbance (258 nm). We determined the minimal quantity of rhodamine B that could be detected from its extremely intense absorbance at 555 nm. The concentration of anilinium was determined from its absorbance (254 nm).
- This work was supported by NSF and the Office of Naval Research.

9 July 1997; accepted 15 September 1997

Femtosecond Mid-IR Pump-Probe Spectroscopy of Liquid Water: Evidence for a Two-Component Structure

S. Woutersen, U. Emmerichs, H. J. Bakker

A femtosecond mid-infrared pump-probe study of the vibrational and orientational dynamics of the OH-stretching mode of HDO dissolved in D_2O is presented. The orientational relaxation of the HDO molecules was observed to occur on either a very slow or a very fast time scale, with associated time constants of $\tau_R = 13$ picoseconds and $\tau_R = 0.7$ picosecond. It was observed that strongly hydrogen-bonded water molecules only relax through the slow orientational relaxation process, whereas the fast process dominates for weakly hydrogen-bonded molecules. This suggests that, with respect to orientational dynamics, two distinct molecular species exist in liquid water.

Knowledge about the orientational dynamics of water is essential for understanding the (bio)chemical and physical processes that take place in this liquid, notably chemical reactions and solvation. Therefore, the reorientational motion of molecules in liquid water has been extensively studied for over half a century, in particular by such methods as dielectric relaxation (1, 2), terahertz spectroscopy (3, 4), optical

and Raman-induced Kerr-effect spectroscopy (5, 6), and nuclear magnetic resonance (7). However, all of the experimental techniques employed to date have probed the orientational motion indirectly or as averaged over all the molecules in the liquid. In contrast, polarization-resolved pump-probe spectroscopy yields unambiguous information about the dynamics of orientational relaxation of small molecules in the liquid phase (8, 9). By developing a laser setup that generates intense femtosecond mid-infrared (mid-IR) pulses, we could study for

FOM—institute for Atomic and Molecular Physics, Kruislaan 407, 1098 SJ Amsterdam, Netherlands.